



Displacement-sensitive photonic crystal structures based on guided resonance in photonic crystal slabs

Wonjoo Suh, M. F. Yanik, Olav Solgaard, and Shanhui Fan

Citation: [Applied Physics Letters](#) **82**, 1999 (2003); doi: 10.1063/1.1563739

View online: <http://dx.doi.org/10.1063/1.1563739>

View Table of Contents: <http://scitation.aip.org/content/aip/journal/apl/82/13?ver=pdfcov>

Published by the [AIP Publishing](#)

Articles you may be interested in

[Numerical investigation of optical Tamm states in two-dimensional hybrid plasmonic-photonic crystal nanobeams](#)
J. Appl. Phys. **116**, 043106 (2014); 10.1063/1.4891222

[Broadband optical characterization and modeling of photonic crystal waveguides for silicon optical interconnects](#)
J. Appl. Phys. **95**, 1606 (2004); 10.1063/1.1630365

[Transmission spectroscopy of photonic crystal based waveguides with resonant cavities](#)
J. Appl. Phys. **91**, 4791 (2002); 10.1063/1.1454199

[Experimental verification of guided modes in 60°-bent defect waveguides in AlGaAs-based air-bridge-type two-dimensional photonic crystal slabs](#)
J. Appl. Phys. **91**, 3477 (2002); 10.1063/1.1436554

[Polymer photonic crystal slab waveguides](#)
Appl. Phys. Lett. **78**, 2434 (2001); 10.1063/1.1366364



Free online magazine

MULTIPHYSICS SIMULATION

READ NOW ►

COMSOL

Displacement-sensitive photonic crystal structures based on guided resonance in photonic crystal slabs

Wonjoo Suh, M. F. Yanik, Olav Solgaard, and Shanhui Fan^{a)}

Department of Electrical Engineering, Stanford University, Stanford, California 94305

(Received 25 November 2002; accepted 3 February 2003)

We introduce a mechanically tunable photonic crystal structure consisting of coupled photonic crystal slabs. Using both analytic theory, and first-principles finite-difference time-domain simulations, we demonstrate that a strong variation of transmission and reflection coefficients of light through such structures can be accomplished with only a nanoscale variation of the spacing between the slabs. Moreover, by specifically configuring the photonic crystal structures, high sensitivity can be preserved in spite of significant fabrication-related disorders. We expect such structures to play important roles in micromechanically tunable optical sensors and filters. © 2003 American Institute of Physics. [DOI: 10.1063/1.1563739]

Microelectrical-mechanical systems (MEMS) technology provides important mechanisms for tuning and switching a wide variety of optical devices such as sensors, filters, modulators, switches, and lasers.^{1–5} The success of these micro-optomechanical devices relies on the fact that the mechanical motion required for their operation is relatively small; on the order of the operating wavelength for high-contrast devices, and only a small fraction of a wavelength for some sensors and lasers. Reducing the required displacement is of great interest in optical MEMS research, because it decreases the required actuation force and enables smaller devices with higher response speed.

In this letter we introduce a MEMS tunable photonic crystal structure that is extremely compact, and yet can achieve high contrast with nanoscale variation in displacement. The structure, as shown in Fig. 1, consists of two photonic crystal slabs. Each slab is constructed by introducing a periodic array of air holes into a high-index guiding layer. We show that a strong variation of transmission and reflection coefficients of light through such structures can be accomplished with only a nanoscale variation of the spacing between the slabs. Moreover, by correct design of the photonic crystal structures, high sensitivity can be preserved in spite of significant fabrication-related disorders.

The operation of the proposed structure relies on the guided resonance phenomena in the slabs.^{6–13} In transmission or reflection spectra, a guided resonance typically manifests itself as a Fano line shape that is superimposed upon a smoothly varying background.^{6–8} In previous work, using a temporal coupled-mode theory, we have shown that the scattering matrix for a single guided resonance can be written in the following general form:¹⁴

$$S = \begin{bmatrix} r & t \\ t & r \end{bmatrix} = \begin{bmatrix} r_d & t_d \\ t_d & r_d \end{bmatrix} + \frac{1/\tau}{j(\omega - \omega_0) + 1/\tau} \begin{bmatrix} -(r_d \pm t_d) & \mp(r_d \pm t_d) \\ \mp(r_d \pm t_d) & -(r_d \pm t_d) \end{bmatrix}, \quad (1)$$

where ω_0 and τ are the center frequency and the lifetime of the resonance, r and t are the transmission and reflection coefficients of the resonator system, and r_d and t_d are the background reflection and transmission coefficients of a corresponding uniform slab at the resonant frequency ω_0 .

For concreteness, we consider a slab with a dielectric constant of 12 and a thickness of $0.55a$ where a is the lattice constant. Within the slab are periodic array of air holes of radius $0.4a$. For such a structure, the theoretical predictions and a finite-difference time domain simulations (FDTD)^{8,15} show excellent agreement.

As can be seen in Fig. 2(a), a distinct property of the guided resonance is the presence of strong reflectivity in the vicinity of ω_0 .¹⁶ Also when the size of the air holes is large, the guided resonance is not a narrow band phenomenon. Rather, strong reflection can occur over a fairly wide range of frequencies. Exploiting this effect, we can construct structures that are highly sensitive to longitudinal displacements by using the photonic crystal slabs as mirrors to form an optical cavity (Fig. 1). When the reflectivity for each slab is high, the transmission becomes highly sensitive to the longitudinal displacements. For transmission through two slabs, the theoretical transmission calculated using Eq. (1) and the standard formula for Fabry-Perot cavity¹⁷ for different values of displacement is shown in Fig. 2(b), and is compared with the FDTD simulations in Fig. 2(c). Having two slabs creates a wider frequency range of near-complete reflection from 0.515 to $0.555(c/a)$. A transmission peak appears within this range with a maximum at 100%. As we reduce the displacement from $1.35a$ to $0.55a$ the peak moves to higher frequencies. The width of the peak depends critically on the reflectivity of a single slab, and can be made arbitrarily small when the frequency peak is in the vicinity of $0.525(c/a)$ at which a single slab shows complete reflection. Therefore, by changing the distance between the slabs we can reconfigure the sensitivity of the structure arbitrarily.

In practice the achievable sensitivity is limited by optical losses especially from absorption and scattering by fabrication-related disorders. For our two-slab structure, the highest achievable sensitivity is directly related to the maximal reflectivity achievable in a single slab. For a single slab,

^{a)}Electronic mail: shanhui@stanford.edu

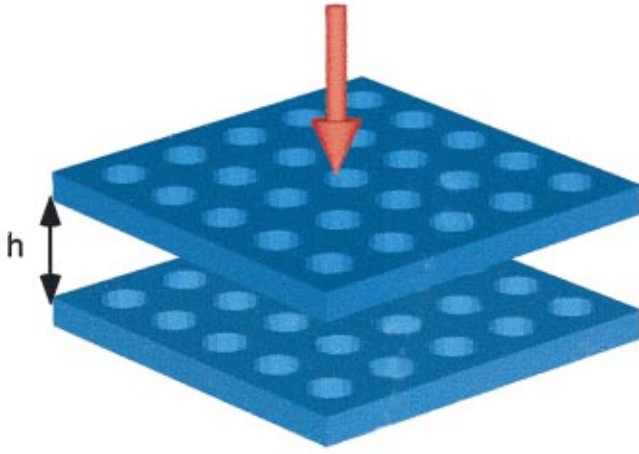


FIG. 1. (Color) Schematic of a displacement-sensitive photonic crystal structure. The structure consists of two photonic crystal slabs. The red arrow represents the direction of the incident light. The transmission spectrum of the normally incident light is strongly influenced by the spacing h between the slabs.

the presence of the disorders reduces the reflectivity by affecting both the direct and the resonance terms in the scattering matrix represented in Eq. (1). However, since strong reflection can only be achieved in the presence of the resonance, our main interest here is to elucidate how optical losses affect the optical resonance. We therefore construct the following simple model, where we incorporate the effect of losses on the resonance in a standard way¹⁸ by introducing an extra decay factor $1/\tau_{\text{loss}}$ into the resonance term in Eq. (1):

$$S = \begin{bmatrix} r & t \\ t & r \end{bmatrix} = \begin{bmatrix} r_d & t_d \\ t_d & r_d \end{bmatrix} + \frac{1/\tau}{j(\omega - \omega_0) + 1/\tau + 1/\tau_{\text{loss}}} \times \begin{bmatrix} -(r_d \pm t_d) & \mp(r_d \pm t_d) \\ \mp(r_d \pm t_d) & -(r_d \pm t_d) \end{bmatrix}. \quad (2)$$

The sensitivity of the two-slab structure can then be estimated starting from Eq. (2). Defining the sensitivity as the minimum displacement δh needed to switch the transmission coefficients from 20% to 80%, we plot δh in Fig. 3(a) as a function of τ/τ_{loss} . In the presence of loss, the sensitivity of the structure becomes finite since the maximum reflectivity from a single slab no longer goes to unity.

The simple model, as represented in Eq. (2), immediately suggests two ways to design structures that are robust against disorders. First of all, it is beneficial to increase the background reflectivity r_d , since doing so enhances the total reflectivity of the structure. This can be accomplished by choosing the appropriate thickness of the slab. In Fig. 3(a), we compare the sensitivity for the case where $r_d(\omega_0) = 0$ and for the case where $r_d(\omega_0)$ is maximized at 0.85. (This value is appropriate for a silicon photonic crystal slab suspended in air).⁸ For the same scattering loss, the structure with a maximal background reflectivity is at least five times more sensitive.

We also note that the effect of optical loss on the resonance enters as a function of τ/τ_{loss} . For a given scattering

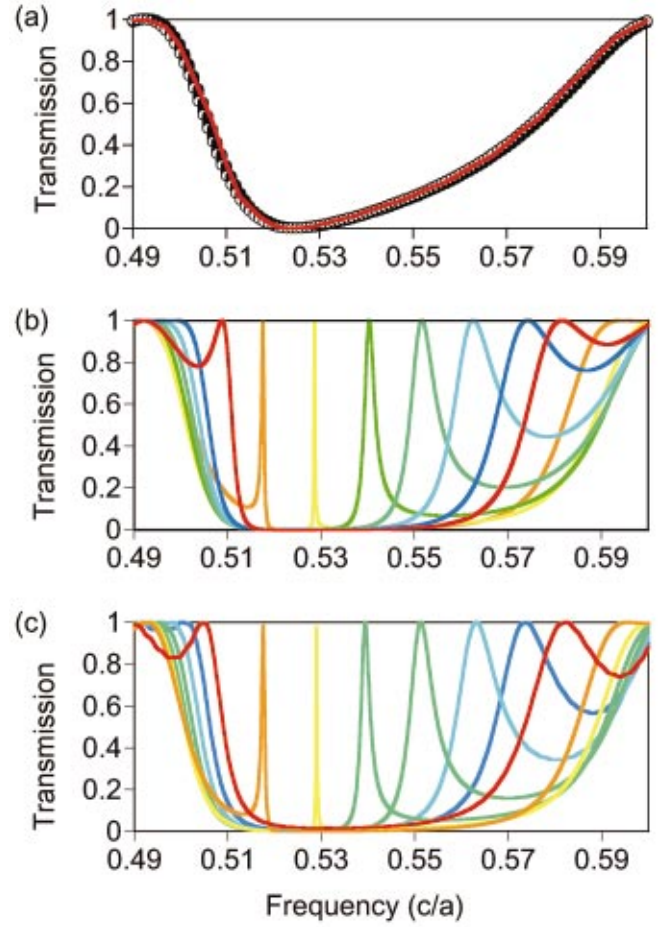


FIG. 2. (Color) (a) Transmission spectrum through a single photonic crystal slab for normally incident light. The crystal structure consists of a square lattice of air holes of radius $0.4a$, where a is the lattice constant, introduced into a dielectric slab. The slab has a dielectric constant of 12 and a thickness of $0.55a$. The open circles are the numerical results from a FDTD simulation. The solid line is a theoretical fit using Eq. (1). (b) Theoretical transmission spectra for a two-slab structure. Each slab is the same as in (a). The colors of the solid lines, varying from red to blue, represent the spacing h between the slabs of $1.35a$, $1.1a$, $0.95a$, $0.85a$, $0.75a$, $0.65a$, and $0.55a$, respectively. The parameters of the theory are taken from the theoretical fit as shown in (a). (c) Transmission spectra for the same two-slab structure as in (b), calculated using FDTD simulations.

lifetime τ_{loss} , we can therefore reduce its effect by decreasing the lifetime τ of the guided resonance in the underlying perfectly periodic lattice. Thus, it is beneficial to use structures with a strong in-plane scattering strength, such as structures with large air holes. We confirm this numerically by employing a supercell approximation to model disorders in the FDTD simulations. The computational domain consists of nine unit cells of the crystal. The effect of disorder is simulated by allowing the radii of holes in each unit cell to fluctuate by as much as 5% of the lattice constant while keeping the average dielectric approximately constant. The normalized scattering loss τ/τ_{loss} is then determined by comparing the lifetimes of the guided resonance between the disordered and the perfect structures, and is shown in Fig. 3(b). Increasing the radius of the holes indeed dramatically reduces the effect of the scattering losses by several orders of magnitude. Combining Figs. 3(a) and 3(b), we estimate that for a crystal structure with the radius of $0.4a$, the achievable sensitivity can be as small as about 1% of the operating

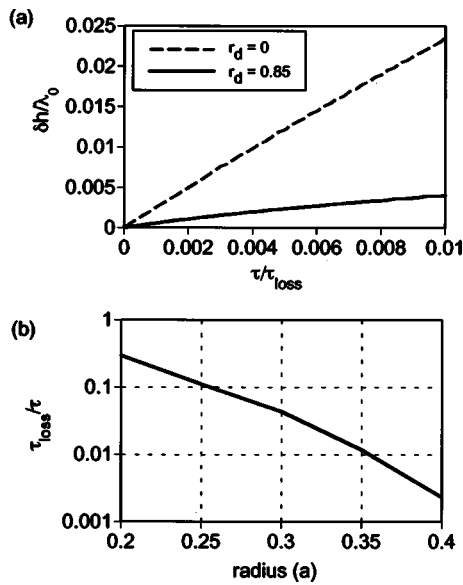


FIG. 3. (a) Sensitivity of the two-slab structure as a function of normalized scattering loss τ/τ_{loss} . The sensitivity is defined as the variation of the spacing between the slabs needed in order to switch the transmission coefficients from 20% to 80%. The solid and the dashed lines correspond to the case of where the background reflection coefficients r_d are 0.85 and 0, respectively. (b) Normalized scattering loss τ/τ_{loss} in disordered photonic crystal slab structures as a function of the radius r_0 of air holes in the underlying perfect lattice. The disorder is introduced by varying the radius of air holes randomly around r_0 in a perfect crystal by as much as $0.05a$, while maintaining approximately the same average dielectric constant.

wavelength. For switching applications, in order to accomplish a 20 dB contrast ratio, the needed shift in displacement h is about 2% of the operating wavelength.

In addition to the longitudinal displacement sensing, the properties of guided resonance also provide opportunities for lateral displacement sensing. For this purpose, one needs to explore the regime of evanescent coupling between the slabs. When $h > 0.5a$, the coupling between the slabs is primarily due to propagating waves. In this far-field coupling regime, the transmission spectra are independent of the lateral alignments of the two slabs. For smaller spacing, evanescent tunneling and near-field coupling between the slabs become important. Figure 4 shows the transmission spectra through the two-slab structures for which the spacing between the slabs $h = 0.1a$. As indicated in Fig. 2(a), each slab supports a resonance around $\omega = 0.53(c/a)$. The near-field coupling between the slabs splits the resonance, leading to strong reflections at $0.524(c/a)$ and $0.555(c/a)$. In addition, a lateral shift of $0.05a$ along the (10) direction breaks the 90° rotational symmetry of the structure, and introduces extra resonances at $0.540(c/a)$ and $0.566(c/a)$. Such resonances correspond to the singly degenerate states that are uncoupled^{8,19} when the two slabs are aligned. The calculation thus demonstrates that the near-field coupling regime provides the additional possibility of lateral displacement sensing.

As final remarks, we note that using the guided resonance phenomenon, high reflectivity can be achieved in a single dielectric layer. This is important in MEMS structures where the mass, size, and internal material stresses of multilayer dielectric stacks often create significant difficulties. Moreover, the high sensitivity to displacement will en-

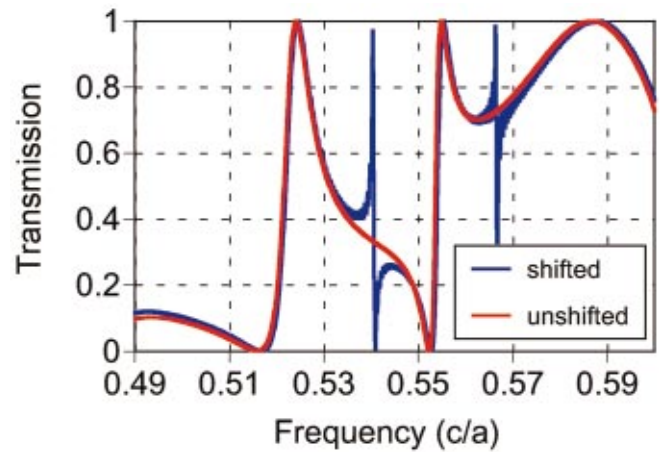


FIG. 4. (Color) Transmission spectra through two-slab structures. Each slab is the same as in Fig. 2(a). The spacing between the slabs is $0.1a$. The red curve corresponds to a structure with holes in two slabs aligned to each other vertically. The blue curve corresponds to a structure with the lattice of holes in the top slab shifted by a distance of $0.05a$ along the (10) direction with respect to the bottom slab.

able MEMS devices with higher speed and lower actuation voltages. The structures proposed here thus provide a tool for optical engineering on the nanoscale.

The simulations were made possible through the NSF National Program for Advanced Computational Infrastructures (NPACI).

- ¹N. C. Loh, M. A. Schmidt, and S. R. Manalis, *J. Microelectromech. Syst.* **11**, 181 (2002).
- ²G. B. Hocker, D. Youngner, E. Deutsch, A. Vol Volpicelli, S. Senturia, M. Butler, M. Sinclair, T. Plowman, and A. J. Ricco, *Technical Digest. Solid-State Sensor and Actuator Workshop*, Hilton Head Island, SC, 4–8 June 2000, pp. 89–92.
- ³O. Solgaard, F. S. A. Sandejas, and D. M. Bloom, *Opt. Lett.* **17**, 688 (1992).
- ⁴P. M. Hagelin, U. Krishnamoorthy, J. P. Heritage, and O. Solgaard, *IEEE Photonics Technol. Lett.* **12**, 882 (2000).
- ⁵C. J. Chang-Hasnain, *IEEE J. Sel. Top. Quantum Electron.* **6**, 978 (2000).
- ⁶M. Kanskar, P. Paddon, V. Pacradouni, R. Morin, A. Busch, J. F. Young, S. R. Johnson, J. Mackenzie, and T. Tiedje, *Appl. Phys. Lett.* **70**, 1438 (1997).
- ⁷V. N. Astratov, I. S. Culshaw, R. M. Stevenson, D. M. Whittaker, M. S. Skolnick, T. F. Krauss, and R. M. De La Rue, *J. Lightwave Technol.* **17**, 2050 (1999).
- ⁸S. Fan and J. D. Joannopoulos, *Phys. Rev. B* **65**, 235112 (2002).
- ⁹M. Boroditsky, R. Vrijen, T. F. Krauss, R. Coccioli, R. Bhat, and E. Yablonovitch, *J. Lightwave Technol.* **17**, 2096 (1999).
- ¹⁰A. Erchak, D. J. Ripin, S. Fan, P. Rakich, J. D. Joannopoulos, E. P. Ippen, G. S. Petrich, and L. A. Kolodziejski, *Appl. Phys. Lett.* **78**, 563 (2001).
- ¹¹H. Y. Ryu, Y. H. Lee, R. L. Sellin, and D. Bimberg, *Appl. Phys. Lett.* **79**, 3573 (2001).
- ¹²M. Meier, A. Mekis, A. Dodabalapur, A. A. Timko, R. E. Slusher, and J. D. Joannopoulos, *Appl. Phys. Lett.* **74**, 7 (1999).
- ¹³S. Noda, M. Yokoyama, M. Imada, A. Chutinan, and M. Mochizuki, *Science* **293**, 1123 (2000).
- ¹⁴S. Fan, W. Suh, and J. D. Joannopoulos, *J. Opt. Soc. Am. A* (to be published).
- ¹⁵K. S. Kunz and R. J. Luebbers, *The Finite-Difference Time-Domain Methods for Electromagnetics* (CRC Press, Boca Raton, FL, 1993); A. Taflov and S. Hagness, *Computational Electrodynamics: The Finite-Difference Time-Domain Methods* (Artech House, Boston, 2000).
- ¹⁶R. Magnusson and S. S. Wang, *Appl. Phys. Lett.* **61**, 1022 (1991).
- ¹⁷B. E. A. Saleh and M. C. Teich, *Fundamentals of Photonics* (Wiley, New York, 1991).
- ¹⁸H. A. Haus, *Waves and Fields in Optoelectronics* (Prentice Hall, Englewood Cliffs, NJ, 1984).
- ¹⁹T. Ochiai and K. Sakoda, *Phys. Rev. B* **63**, 125107 (2001).